PROCEEDINGS OF SCIENCE

Highlights and perspectives from the ATLAS Experiment

Manuella G. Vincter[a,*] **on behalf of the ATLAS Collaboration**

[a] *Carleton University,*
1125 Colonel By Drive, Ottawa, ON, K1S 5B6, Canada

E-mail: vincter@physics.carleton.ca

The ATLAS Experiment is preparing for the upcoming Run 3 of CERN's Large Hadron Collider, while at the same time fully exploiting the abundant and now well-understood Run-2 dataset. A wide range of measurements and searches employing the full Run-2 dataset is presented, including results in the areas of heavy-ion, top-quark, di-boson, and Higgs boson physics, as well as searches beyond the Standard Model. Some highlights of the ongoing improvements targeting Run 3 are also presented.

The Ninth Annual Conference on Large Hadron Collider Physics - LHCP2021
7-12 June 2021
Online

*Speaker

PoS(LHCP2021)106

1. Introduction

The ATLAS Experiment [1] based at the Large Hadron Collider (LHC) at the CERN laboratory is preparing for the upcoming Run-3 data-taking period starting in March 2022, while simultaneously exploiting the rich harvest of LHC collisions recorded during Run 2 in 2015–2018. The results presented here are based on the full Run-2 data-taking period, which represents a very well understood proton–proton dataset with precision object reconstruction and identification performance, such as knowledge of the jet-energy scale in the central region of ATLAS at the 1% level over much the kinematic range, as well as dedicated heavy-ion running periods. At the time of the LHCP2021 conference, approximately 135 full Run-2 ATLAS results were available, including approximately 90 submitted for publication.

2. Heavy-ion physics

Particles lose energy as they traverse the nuclear medium arising from heavy-ion collisions. An expected suppression at low transverse momentum, p_{T}, of small-angle gluon radiation for massive quarks may be probed by measuring the nuclear modification factor, R_{AA}, a quantity that compares the particle yields for proton–proton and heavy-ion (in this case, Pb-Pb) scattering as a function of the centrality of the event. A suppression in R_{AA} is observed to increase monotonically from the more peripheral to the more central collisions for events containing either a b or c quark decaying a muon [2]. The ratio of these nuclear modification factors, $R_{AA}^{\mathrm{charm}}/R_{AA}^{\mathrm{bottom}}$, shown in Fig. 1 (left), does indeed indicate a modification at low-p_{T}, as expected from predictions.

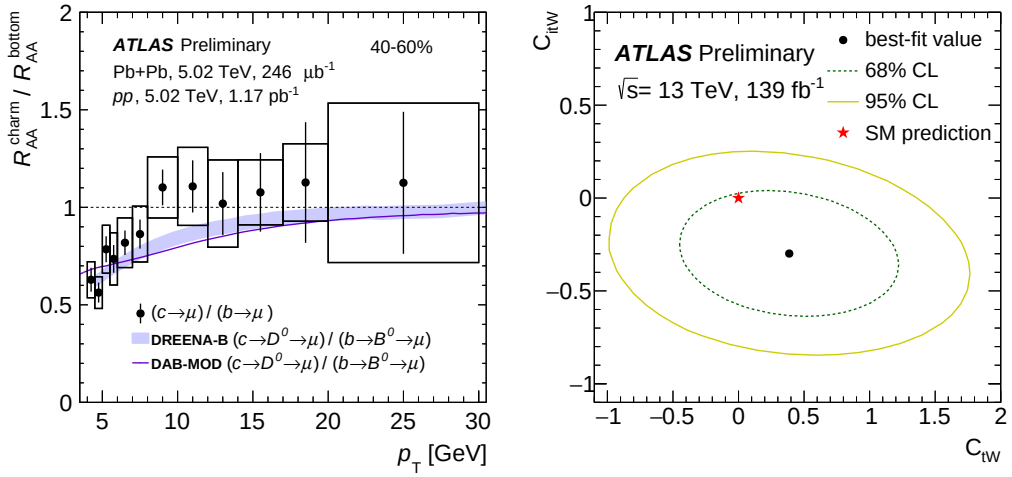

Figure 1: Left: The ratio of $c \to \mu$ and $b \to \mu$ R_{AA} for Pb-Pb collisions with a centrality of 40–60%, plotted as a function of muon p_{T} [2]. Right: The observed best-fit value for the real (x-axis) and imaginary (y-axis) components of the Wilson coefficients C_{tW} in EFT plotted with the uncertainty contours at 68% (dashed) and 95% (solid) confidence level (CL). The red star indicates the Standard Model prediction [4].

3. Standard Model physics

The large Run-2 dataset enables ATLAS to look for very rare collision events, *e.g.*, the simultaneous production of four top quarks in an event, which may be used to probe the top-Higgs Yukawa coupling. The analysis [3], performed with one-lepton and two-lepton (opposite-charge) final states (a significant 57% of all expected $t\bar{t}t\bar{t}$ events, but which suffers from copious $t\bar{t}$ background) is combined with the cleaner but less abundant two-lepton (same-charge) and three-lepton final states (13% of all expected $t\bar{t}t\bar{t}$ events), resulting in an observed (expected) 4.7 (2.6) standard-deviation significance above the background-only hypothesis.

Single-top-quark production in the t channel, a once rare process but now quite abundant process due to to large Run-2 dataset, may be used to probe the tWb interaction vertex. The nature of this vertex implies that the polarisation of the top quark should be aligned mostly along the direction of motion of the spectator quark. The spin information of the top quark is then transmitted to the angular distribution of its decay products. In this analysis [4], the three components of polarisation vector are simultaneously extracted. Such information has sensitivity to possible new physics occurring in the tWb vertex, which may be extracted by measuring the real and imaginary components of the Wilson coefficient C_{tW} in the framework of an Effective Field Theory (EFT) through the x and y components of the polarisation vector. As shown in Fig. 1 (right), the results are very consistent with the Standard Model prediction.

The Run-2 dataset is also used to probe Electroweak and QCD interactions at the highest energy scales. The differential cross section of $W^{\pm}W^{\mp}$ production decaying to an electron and a muon and with at least one jet in the final state is measured with an uncertainty of 10% as a function of variables that characterise W kinematics and jet production [5]. The requirement of one hard jet ($p_{\mathrm{T}} > 200$ GeV) in the event improves the sensitivity to searches for anomalous triple-gauge-boson couplings (aTGCs); such quantities are studied in a dedicated phase-space in order to constrain the Wilson coefficient, C_W, in EFT.

4. Higgs-boson physics

The production of two W bosons is also used to probe the properties of the Higgs boson produced via gluon fusion (ggF) and vector-boson fusion (VBF) [6]. The background composition depends very much on the number of jets N_{jet} in the final state. For VBF production, a deep neural network is used in the $N_{\mathrm{jet}} \geq 2$ phase space to demonstrate a very convincing signal with a 6.6 (6.1) standard-deviation observed (expected) significance above the background-only hypothesis. For ggF production, nearly 4 000 $H \rightarrow W^{+}W^{-}$ events are observed as a function of the transverse mass m_{T}, extracted from the $N_{\mathrm{jet}} = 0, 1, \geq 2$ categories. A two-dimensional plot of the cross section times the branching fraction for these two processes shows excellent agreement with the Standard Model prediction.

One of the next experimental challenges to confirm the Standard Model nature of the Higgs boson is to measure its coupling to second-generation quarks; the branching fraction for $H \rightarrow c\bar{c}$ is 20 times smaller than that for $H \rightarrow b\bar{b}$, making it a challenging channel to investigate. In this analysis [7], $H \rightarrow c\bar{c}$ is measured in association with a vector boson V (W or Z) decaying to one or two light leptons (e or μ). A maximum-likelihood fit is performed to the $c\bar{c}$ invariant mass,

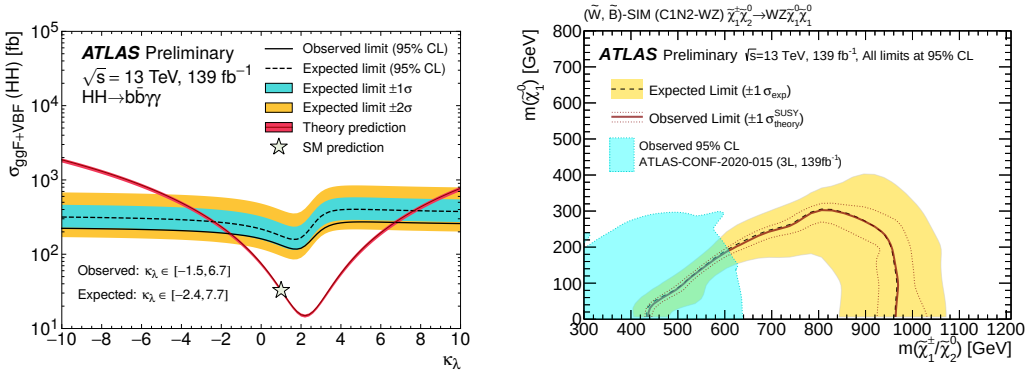

Figure 2: Left: Observed and expected limits at 95% confidence level on the cross section of non-resonant Higgs-boson-pair production as a function of the Higgs-boson self-coupling modifier $\kappa_\lambda = \lambda_{HHH}/\lambda^{SM}_{HHH}$ [8]. Right: Exclusion limits as a function of the produced wino mass $m_{\tilde{\chi}^\pm_1/\tilde{\chi}^0_2}$ and the bino LSP mass $m_{\tilde{\chi}^0_1}$ interpreted in the C1N2-WZ simplified model [11].

revealing no excess of events near the expected Higgs-boson mass. This information is used to extract an upper limit on the Standard Model signal strength of $\mu = 26$ times the Standard Model cross section for $VH(c\bar{c})$. This information is also interpreted in the Kappa framework to extract upper limits on the Yukawa coupling modifier strength of $|\kappa_c| < 8.5$ at 95% confidence level. This result represents the most stringent constraint to date on this quantity.

The ultimate study to probe the structure of the Higgs potential is to measure the Higgs-boson self-interaction, the *raison d'être* of the High Luminosity LHC (HL-LHC). Such a quantity is already probed with the full Run-2 dataset, with the search for $HH \to b\bar{b}\gamma\gamma$ production [8]. Once again, the two major production mechanisms considered are ggF and VBF. The non-resonant search uses four event categories and performs a fit to the invariant mass of the di-photon system. This information is used to extract upper limits on the cross section of 4.1 observed (5.5 expected) times the Standard Model expectation and is used to evaluate the Higgs-coupling modifier κ_λ, which is the ratio of the Higgs-boson self-coupling to its Standard Model value. The value of this quantity is now constrained to be between -1.5 and 6.7 at 95% confidence level, see Fig. 2 (left). These results represent an improvement of a factor of five on the upper limit for the signal strength and a factor of two on the constraints for κ_λ.

5. Beyond the Standard Model

The LHC is a critical tool to probe electroweak symmetry breaking. Some scenarios that attempt to address the naturalness problem, also predict the existence of new vector resonances. In a new analysis [9], the decay $W' \to WH \to \ell\nu b\bar{b}$ (where $\ell = e, \mu, \tau$) is searched for using resolved and merged b jets. Excesses beyond Standard Model expectations are searched for with the WH invariant mass. Since none are observed, this information is used to extract upper limits on the cross section of 1.3 pb (0.56 fb) at $m_{W'} = 400$ GeV (5 TeV) and interpreted in two benchmarks of the Heavy Vector Triplet Model; a W' with a mass of ≤ 3 TeV is excluded for both models.

If a W' exists, it could also be observed in other decay modes. An analysis [10] is presented searching for a W' that subsequently decays into a hadronically-decaying τ lepton that is identified

using a recurrent neural network. Profile-likelihood fits are performed on the m_{T} in the visible hadronic τ plus missing transverse energy system. Excellent agreement is observed between the data and the Standard Model expectation. This result is used to extract upper limits on the branching fraction times the cross section and is interpreted in two models: the Sequential Standard Model, which is a flavour universal model with W' couplings to fermions identical to those of W bosons, and Non-Universal Gauge Interaction Models, where lepton universality is violated and there are different couplings for the three lepton generations. In the first (second) model, the W' is excluded for masses up to 5 TeV (3.5-5 TeV) at 95% confidence level.

The LHC is designed to be a discovery machine, and so an area of intense activity within ATLAS is to search for Supersymmetry (SUSY); three results in this area are presented. The first analysis [11] is a search for the pair production of electroweakinos in the fully hadronic final state. In this process, W, Z, or H bosons are produced and decay to either four light quarks, $qqqq$, or two lights quarks and two b quarks, $qqbb$. Large-radius jets are employed to capture the collimated energetic jets of this final state and a powerful jet-substructure technique is used to identify hadronic decays of the W, Z, or H bosons. Ten orthogonal signal regions are used to target these two final states. The results are interpreted in several beyond-the-Standard-Model scenarios. In the case of the Minimal Supersymmetric Standard Model (MSSM) where the bino, wino, and higgsino are heavy and light electroweakinos, wino pair production decaying to bino lightest-supersymmetric particles (LSP) excludes masses m($\tilde{\chi}_1^{\pm}/\tilde{\chi}_2^0$) up to 1 060 GeV for $m_{\tilde{\chi}_1^0} < 400$ GeV in the C1N2-WZ simplified model, see Fig. 2 (right). This result represents a significant improvement from previous measurement and is the most stringent limit on this model to date.

The other two SUSY searches presented have non-standard signatures in the detector; they involve long-lived particles decaying within the detector volume. The first analysis [12] is a search for gluinos forming R-hadrons that subsequently stop in the detector for minutes, hours, or even days and then decay isotropically leaving significant out-of-time energy deposits in the calorimeter not associated to proton–proton collisions. Such a signature is challenging to analyse as empty LHC bunches must be used for triggering and non-standard (cosmics) reconstruction used for the particles detected. Signal regions are built based on leading-jet $|\eta|$ and p_{T}, and interpreted in several scenarios that depend on the mass of the lightest neutralino or the mass difference between the gluino and the lightest neutralino. This analysis excludes the existence of gluinos with masses of $0.6 - 1.4$ TeV, for gluino lifetimes ranging from the first empty LHC bunch crossing after the collision to approximately one year. A search for long-lived charginos is also performed [13], produced either through direct electroweak production or via a strong cascade. Such a chargino could live long enough to traverse multiple layers of the ATLAS Pixel detector before decaying into a neutralino and a charged pion, neither of which would be observed in the detector. The signature is thus a disappearing track early in the inner detector, and no other activity in the inner detector nor in the calorimeter; a significant amount of missing transverse energy is also expected in the final state along with high p_{T} jets, particularly for the case of strong production. Two signal regions are built targeting the two production mechanisms. The results are interpreted in SUSY scenarios with wino and higgsino LSP. For e.g., if the chargino $\tilde{\chi}_1^{\pm}$ is pure wino, chargino masses up to 660 GeV are excluded. If on the other hand it is pure higgsino, chargino masses up to 210 GeV are excluded.

The LSP of the SUSY searches presented above are viable candidates for dark matter. Dark matter is known to exist in the Universe, though what form it takes is at the moment unknown.

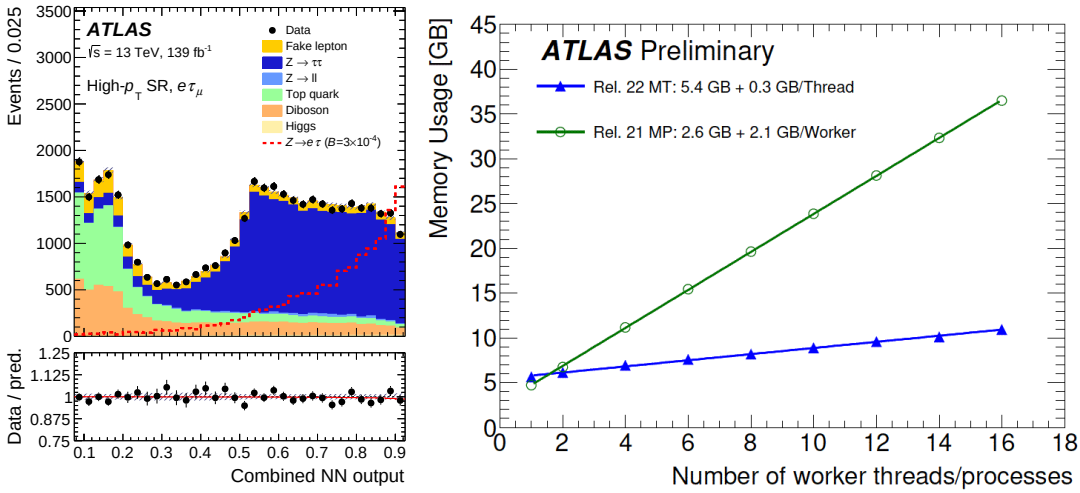

Figure 3: Left: Observed and best-fit predicted distributions of the combined neural-network output in the high-p_{T} signal region for the $e\tau_\mu$ final state. The expected signal, normalised to an arbitrary $B(Z \to \ell\tau) = 3 \times 10^{-4}$ is also plotted [15]. Right: Memory usage of the multi-threaded reconstruction as a function of the number of threads in the new Release 22 (blue triangles) compared to that of the multi-process reconstruction as a function of the number of workers in the previous Release 21 (open green circles) [16].

Searching for dark-matter production at the LHC is one of ATLAS' important research priorities. The analysis [14] presented is a search for dark matter produced in association with a Higgs boson decaying to a $b\bar{b}$ final state. The signature for such a final state is missing transverse energy (arising from the dark matter), merged or resolved b jets and potentially other associated jets. The result probes a Higgs boson coupling directly to dark matter, or via an intermediate beyond-the-Standard-Model particle. The result is interpreted in the Two-Higgs-Doublet Model (2HDM) where there are two neutral scalars (a CP-even h with mass 125 GeV and a CP-odd A). The two simplified benchmark models employed in the 2HDM, extended by dark-matter particles, are the Z'-2HDM and the 2HDM+a, where a is a pseudoscalar singlet. Excellent agreement with the Standard Model expectation is observed in the $b\bar{b}$ invariant mass, thereby ruling out in the first model $m_{Z'}$ up to 3.1 TeV for $m_A = 300$ TeV and in the second model m_a up to 520 GeV for $m_A = 1.25$ TeV (in both cases, for the ratio of neutral Higgs field vacuum expectation values of $\tan\beta = 1$).

The final measurement presented is a probe of lepton-flavour universality [15]. Lepton flavour is conserved in the Standard Model but it's not protected by any fundamental principle. Its violation has been observed in neutrino oscillations, but so far there are no indications of violations in the charged sector. The analysis presented is a search for the decay $Z \to \ell\tau_{\ell'}$, where $\ell, \ell' = e, \mu$. Three neural network binary classifiers are used as input into the combined output. A maximum-likelihood fit is performed in signal regions of high and low p_{T}. As shown in Fig. 3 (left), excellent agreement between the data and the Standard Model prediction is observed. The results are combined with a previous search using hadronic decays of the τ in $Z \to \ell\tau_{had}$. Together, these two results form the most stringent constraint to date on lepton-flavour violation using Z-boson decays involving τ; the branching-fraction limit is set to $B(Z \to \ell\tau) < 5 - 8 \times 10^{-6}$.

Figure 4: All of ATLAS is getting ready for Run 3.

6. Preparing for Run 3

This presentation concludes with an overview of some of the activities ongoing as ATLAS gets ready for Run 3. A huge effort was undertaken to enable early Run-3 data combinations with Run-2 data. ATLAS is moving to a single lightweight but flexible data format. The software has migrated to multi-threaded mode, showing huge gains in the memory usage per thread [16], as seen in Fig. 3 (right). Run-3 trigger strategies and algorithms are being finalised, and a multi-year programme to have a new, more performant fast simulation is concluding.

Whether it be essential detector maintenance for Run 3 or the completion of detector upgrades that will enable new functionality, especially for the HL-LHC, ATLAS wishes to take full advantage of the many improvements in the works. Such improvements include at the Level-1 Trigger a finer granularity of the Liquid Argon Calorimeter readout and feature extractors to enable new event topologies. The installation of the New Small Wheels muon chambers in the forward regions of the detector, targeting the reduction of trigger rates of muons not pointing to the interaction region, is the largest new detector component to be installed within ATLAS since its construction; it should be finalised in time for Run 3.

7. Summary

A full range of proton–proton and heavy-ion physics results from the ATLAS Experiment at the LHC are presented, including the 4.7 standard deviation evidence for four-top-quark production, the observations of thousands of $H \rightarrow WW$ events, significant improvements on the limits for di-Higgs production, new tighter constraints on the search for long-live particles, and the most stringent constraints to date on lepton-flavour violation searches involving Z bosons decaying to τ. The preparations for Run 3 are in full swing, see Fig. 4!

References

[1] ATLAS Collaboration, JINST **3** (2008) S08003, http://iopscience.iop.org/article/10.1088/1748-0221/3/08/S08003/meta.

[2] ATLAS Collaboration, ATLAS-CONF-2021-020, http://cdsweb.cern.ch/record/2766615.

[3] ATLAS Collaboration, http://arxiv.org/abs/2106.11683.

[4] ATLAS Collaboration, ATLAS-CONF-2021-027, http://cdsweb.cern.ch/record/2773738.

[5] ATLAS Collaboration, JHEP **06** (2021) 003, http://link.springer.com/article/10.1007/JHEP06(2021)003.

[6] ATLAS Collaboration, ATLAS-CONF-2021-014, http://cdsweb.cern.ch/record/2759651.

[7] ATLAS Collaboration, ATLAS-CONF-2021-021, http://cdsweb.cern.ch/record/2771724.

[8] ATLAS Collaboration, ATLAS-CONF-2021-016, http://cdsweb.cern.ch/record/2759683.

[9] ATLAS Collaboration, ATLAS-CONF-2021-026, http://cdsweb.cern.ch/record/2773302.

[10] ATLAS Collaboration, ATLAS-CONF-2021-025, http://cdsweb.cern.ch/record/2773301.

[11] ATLAS Collaboration, ATLAS-CONF-2021-022, http://cdsweb.cern.ch/record/2772663.

[12] ATLAS Collaboration, JHEP **07** (2021) 173, http://link.springer.com/article/10.1007/JHEP07(2021)173.

[13] ATLAS Collaboration, ATLAS-CONF-2021-015, http://cdsweb.cern.ch/record/2759676.

[14] ATLAS Collaboration, ATLAS-CONF-2021-006, http://cdsweb.cern.ch/record/2759211.

[15] ATLAS Collaboration, http://arxiv.org/abs/2105.12491.

[16] ATLAS Collaboration, ATLAS-SOFT-PUB-2021-002, http://cdsweb.cern.ch/record/2771777.